NIH Public Access
Author Manuscript
J Am Chem Soc. Author manuscript; available in PMC 2009 December 31.

Published in final edited form as:
J Am Chem Soc. 2008 December 31; 130(52): 17858–17866. doi:10.1021/ja8059864.

An Altered Transition State for the Reaction of an RNA Model Catalyzed by a Dinuclear Zinc(II) Catalyst

Tim Humphry[†,a], **Subashree Iyer**[†,b], **Olga Iranzo**[‡,c], **Janet R. Morrow**[‡], **John P. Richard**[‡], **Piotr Paneth**[¶], and **Alvan C. Hengge**[†]

[†]*Department of Chemistry and Biochemistry, Utah State University, Logan Utah 84322-0300* [‡]*Department of Chemistry, University at Buffalo, State University of New York, Buffalo, NY 14260* [¶]*Institute of Applied Radiation Chemistry, Technical University of Lodz, Zeromskiego 116 Zeromskiego 116, 90-924 Lodz, Poland*

Abstract

The cyclization of 2-hydroxypropyl-4-nitrophenyl phosphate (HpPNP) catalyzed by the dinuclear zinc complex of 1,3-bis(1,4,7-triazacyclonon-1-yl)-2-hydroxypropane (**1**) proceeds by a transition state that is different from that of the uncatalyzed reaction. Kinetic isotope effects (KIEs) measured in the nucleophilic atom and in the leaving group show that the uncatalyzed cyclization has a transition state (TS) with little phosphorus-oxygen bond fission to the leaving group ($^{18}k_{lg}$ = 1.0064 ± 0.0009 and ^{15}k = 1.0002 ± 0.0002), and that nucleophilic bond formation occurs in the rate-determining step ($^{18}k_{nuc}$ = 1.0326 ± 0.0008). In the catalyzed reaction, larger leaving group isotope effects ($^{18}k_{lg}$ = 1.0113 ± 0.0005 and ^{15}k = 1.0015 ± 0.0005) and a smaller nucleophile isotope effect ($^{18}k_{nuc}$ = 1.0116 ± 0.0010) indicate a later TS with greater leaving group bond fission, and greater nucleophilic bond formation. These observed nucleophile KIEs are the combined effect of the equilibrium effect on deprotonation of the 2'-hydroxyl nucleophile and the KIE on the nucleophilic step. An EIE of 1.0245 for deprotonation of the hydroxyl group of HPpNP was obtained computationally. The different KIEs for the two reactions indicate that the effective catalysis by **1** is accompanied by selection for an altered transition state, presumably arising from the preferential stabilization by the catalyst of charge away from the nucleophile and toward the leaving group. These results demonstrate the potential for a catalyst using biologically relevant metal ions to select for an altered transition state for phosphoryl transfer.

Introduction

One of the central functional groups in biology is the phosphodiester linkage of the genetic materials DNA and RNA. The RNA linkage is more susceptible to hydrolysis due to the proximity of the 2' hydroxyl group, which serves as an intramolecular nucleophile. The phosphodiester bond in RNA undergoes fission by the two-step process shown in Scheme 1, in which an intermediate cyclic 2',3'-phosphodiester forms that is subsequently opened by attack of water. This overall mechanism is followed both in the base-catalyzed hydrolysis in solution, as well as by ribonucleases.

The details of the cyclization step, in both the ribonuclease-catalyzed reaction and the base-catalyzed reaction, have been the matter of debate. The cyclization reaction has been studied

Correspondence to: Alvan C. Hengge, alvan.hengge@usu.edu.

[a]Present affiliation: Chemistry Department, Gonzaga University, Spokane, WA 99258
[b]Present affiliation: Albany Molecular Research, Inc. Albany, NY 12212
[c]Present affiliation: Instituto de Tecnologia Química e Biológica, Portugal

NIH-PA Author Manuscript
NIH-PA Author Manuscript
NIH-PA Author Manuscript

NIH-PA Author Manuscript

NIH-PA Author Manuscript

NIH-PA Author Manuscript

using ribose-3'- alkyl and aryl phosphates (A, Figure 1) , and with model systems such as 2-hydroxypropyl-aryl phosphates (B, Figure 1).[1–5]

Two studies using linear free energy relationships (LFER) have examined the mechanism for the cyclization of uridine-5'phosphoesters (A in Figure 1). In a study using aryl ester leaving groups, LFER results were interpreted as supporting a concerted mechanism.[1] Subsequently, the observation of a more negative Brønsted β_{lg} for alkyl esters (−1.28, versus −0.54 for aryl esters) was taken as evidence for a stepwise reaction with a discrete phosphorane intermediate; the rate-limiting step was proposed to be formation of the intermediate for aryl leaving groups, and breakdown for alkyl leaving groups.[4] A β_{lg} of −0.56 was measured[2] for the hydrolysis of 2-hydroxypropyl-aryl phosphates (B), very similar to the value of −0.54 for uridine-3'-arylphosphates, evidence that the two classes of compounds cyclize with a similar mechanism and transition state.

This reaction is effectively catalyzed by the di-Zn(II) complex **1**, which functions as a catalyst for the hydrolysis of activated ribonucleotide analogs such as 2-hydroxypropyl-4-nitrophenyl phosphate (HpPNP; Figure 1B, Ar = *p*-nitrophenyl) and uridine-3'-*p*-nitrophenylphosphate (UpPNP), as well as physiological dinucleotides such as UpU.[6,7] Complex **1** is a potent catalyst in which the two metal cations function cooperatively[8] to stabilize the transition state for the cyclization of HpPNP by 9.3 kcal/mol.[6] Kinetic data support a mechanism in which the zinc-bound hydroxide functions as a base to deprotonate the secondary hydroxyl nucleophile, and the absence of a significant solvent deuterium isotope effect implies that no proton is in flight in the rate-determining step.[9] This indicates that deprotonation occurs in a preequilibrium step before nucleophilic attack, as shown in Figure 2.

A longstanding issue in enzymatic catalysis in general, and in phosphate ester catalysis in particular, is whether enzymes select for altered transition states relative to their corresponding uncatalyzed reactions. It is intuitively attractive to assume that metal ions or cationic side chains at enzymatic active sites might render the transition state for phosphoryl transfer more associative.[10] This would be analogous to the change that results from alkyl substitution: transition states for hydrolysis become more associative in the continuum from monoesters to triesters. In metal-catalyzed phosphoryl transfer reactions, the effect of metal ions on mechanism and transition state has been found to vary. In solution, added magnesium and calcium ions do not alter the loose transition state for the hydrolysis of aryl phosphate monoesters[11] or of ATP.[12] The kinetics of reactions of *p*-nitrophenyl phosphate coordinated monodentately to mononuclear Co(III) complexes are consistent with either a concerted process or an addition-elimination mechanism.[13] Kinetic isotope effect (KIE) data with such complexes[14] are more consistent with a concerted mechanism and a transition state not significantly different from the uncatalyzed hydrolysis. In these complexes phosphoryl transfer is to an adjacent, coordinated nucleophile. The best-studied metallophosphatase, alkaline phosphatase, operates via a transition state not significantly different from the uncatalyzed hydrolysis.[15,16]

The mechanistic consequences of metal ion catalysis in reactions of phosphodiesters have been less thoroughly investigated. Diesters coordinated to a dinuclear Co(III) complex undergo reaction by a two-step mechanism in which nucleophilic attack by a bridging oxo nucleophile to form a coordinated phosphorane intermediate is followed by rate-limiting breakdown involving bond fission to the leaving group, in contrast to the concerted mechanism followed by the uncomplexed diesters.[17,18] These results demonstrate the potential for metal ion complexation to alter the mechanism of diester hydrolysis. Another dinuclear zinc catalyst, a methoxide-bridged dinuclear Zn(II) complex of 1,3-[N, N'- bis(1,5,9-triazacyclododecane)] propane, has been shown to be a highly efficient catalyst in methanol solution for the cyclization of HpPNP and other aryl esters of type B of Figure 1.[19] This catalyst is structurally similar to

NIH-PA Author Manuscript

NIH-PA Author Manuscript

NIH-PA Author Manuscript

1 but lacks the bridging alkoxide ligand. In its reactions, the rate-limiting step for poorer substrates is the chemical step of cyclization, while for more activated substrates such as HpPNP, the rate-limiting step is coordination to the complex.[19] Mg^{2+} ribonuclease P ribozyme-catalyzed RNA cleavage shows a nucleophile KIE similar to that for Mg^{2+}-catalyzed diester cleavage, implying similar transition state and concerted mechanisms in both reactions.[20]

In this study, we examine how the mechanism and transition state for the cyclization of HpPNP catalyzed by **1** compares with the uncatalyzed cyclization. Heavy-atom KIEs were measured in three positions for the catalyzed cyclization and for the uncatalyzed specific base reaction. The ^{18}O KIEs were measured in the nucleophilic and in the scissile oxygen atoms, and the ^{15}N KIE in the leaving group. The KIEs permit an analysis of the extent of nucleophile bond formation, and leaving group bond fission and charge development, in the transition state. Comparisons of these parameters between the catalyzed and uncatalyzed reactions permit a direct comparison of the transition states. The ^{18}O KIEs were measured by the remote label method using the nitrogen atom in the *p*-nitrophenyl leaving group as a reporter for the oxygen ratios. Since the leaving group departs in the cyclization step and is unaffected by the subsequent ring-opening hydrolysis, the KIEs reflect the transition state for the cyclization step, regardless of whether cyclization or the subsequent ring-opening is rate-limiting for the overall reaction.

Materials and Methods

Syntheses

Triethylamine was distilled from BaO, and THF distilled under nitrogen from sodium just before use. All other commercial solvents and reagents were used as received. [$^{18}O_2$]-Benzoic acid[21] and [^{15}N]-*p*-nitrophenyl phosphorodichloridate[22] were made using previously published procedures.

Natural abundance and bridge-labeled isotopic isomers of HpPNP were made using a slight adaptation of a previously published procedure[5] which was in turn adapted from the original synthetic procedure.[2] The procedure used is illustrated in the following example: 11 mL of propylene oxide (157 mmol) and 360 mg (0.828 mmol) of the di-cyclohexylammonium salt of *p*-nitrophenyl phosphate (*p*-NPP) were stirred vigorously at 30°C in 10 mL of water in a capped round bottom flask. The reaction progress was monitored by ^{31}P NMR, and stopped before the hydrolysis product began to appear, which was typically ~ three days. The solution was then concentrated to a yellow oil by removal of unreacted propylene oxide by rotary evaporation. Unreacted *p*-NPP was precipitated by adding excess ethanol, and removed by Büchner filtration. The ethanol was removed via rotary evaporation and the remaining yellow oil was diluted with water and eluted through Dowex 50WX8-100 cation exchange resin in the proton form. The acidic fractions (pH ~2) were collected and titrated to pH 6.8 using saturated $Ba(OH)_2$. The resultant light yellow solution was then concentrated via rotary evaporation, again resulting in a thick yellow oil. The final product, the barium salt of HpPNP, was obtained as a white solid by triturating the yellow oil with diethyl ether. The final yield of Ba $(HpPNP)_2$ was 162 mg (0.235 mmoles), or 28%. The proton and phosphorus NMR spectra matched previously reported values for this compound.

Natural abundance HpPNP was used for measurement of the ^{15}N KIE, ^{15}k. The ^{18}O KIEs $^{18}k_{lg}$ and $^{18}k_{nuc}$ were measured by the remote-label method,[23] using the nitrogen atom as a reporter for the oxygen at the position of interest. The correlated pairs of isotopic isomers of HpPNP used for the ^{18}O KIE measurements are shown in Figure 3.

NIH-PA Author Manuscript

NIH-PA Author Manuscript

NIH-PA Author Manuscript

Natural abundance HpPNP for ^{15}N KIE measurements was synthesized using natural abundance *p*-NPP. The leaving group mix was synthesized using *p*-NPP with the necessary correlated isotopic labels already in the correct positions, which was made, in turn, from a mixture of [^{14}N]-*p*-nitrophenol (depleted in ^{15}N) and [^{15}N]-*p*-nitrophen[^{18}O]ol. These labeled nitrophenols were synthesized and phosphorylated as previously described.[24] The nucleophile mix required [^{14}N]-HpPNP which was synthesized as shown in Scheme 2, and 2-[^{18}O] hydroxypropyl-[^{15}N]-*p*-nitrophenyl phosphate, which was synthesized as shown in Scheme 3 and described in detail below.

2-(*t*-butyldiphenylsilyloxy)-1-propanol (3) (Scheme 4)—13.74 g (50.1 mmol) of *t*-butyldiphenylsilyl chloride was dissolved in dry DMF and cooled in an ice bath. To this solution 6.81g (100 mmol) of imidazole was added in one portion. Ethyl (S)-lactate (11.8 g, 100 mmol) was added dropwise, and the solution was stirred for 24h. The reaction was quenched by adding water, the product was extracted into ether and washed with water twice and once with brine. The ether solution was dried over Na_2SO_4, filtered, and concentrated yielding 18 g (99%) of product as a pale yellow oil which was used in the next step without purification. After dissolving the yellow oil in anhydrous THF and cooling in an ice bath, 200 mL of 1.0 M borane•THF complex solution was added dropwise over a period of 0.5 h. After complete addition, the ice bath was removed and the reaction was allowed to attain room temperature. The solution was then refluxed for 3h. The reaction was cooled and quenched by slow addition of water until bubbling ceased. After removal of THF by rotary evaporation the product was dissolved in ether and was washed with water and brine. The ether solution was dried over Na_2SO_4, filtered, and concentrated, yielding 15.2 g of product. This was used in the preparation of **4** (Scheme 2) without further purification. ^1H NMR (300 MHz, $CDCl_3$) δ 1.06 (d, J = 9 Hz, 3H), 1.10 (s, 9H), 2.02 (s, 1H), 3.42–3.52 (m, 2H), 3.95–3.99 (m, 1H), 7.36–7.48 (m, 6H), 7.70–7.75 (m, 4H). ^{13}C NMR δ 19.3, 19.8, 27.1, 68.3, 70.3, 127.7 (d, J = 9.7 Hz), 129.8 (d, J = 5.2 Hz), 139.9 (d, J = 16.5 Hz), 135.8 (d, J = 9 Hz).

2-(*t*-Butyldimethylsilyloxy)-propyl]-*p*-Nitrophenyl phosphate, triethylammonium salt (4)—[^{14}N]- *p*-nitrophenylphosphorodichloridate[22] 1.45 g (6.66 mmoles) was dissolved in dry THF under nitrogen and cooled to 0 °C in an ice bath. 2-(*t*-butyldiphenylsilyloxy)-1-propanol (2.10 g (6.66 mmoles) was dissolved in a vial containing a 10 mL mixture of dry Et_3N and dry THF in a ratio of 1:10. This solution was then added to the *p*-nitrophenyl-phophorodichloridate solution *via* a syringe over a period of 0.5 h. After addition was complete the ice bath was removed and the reaction vessel was allowed to attain RT and stirred for an additional hour. To this solution a 15 mL mixture of Et_3N and water (1:5) was added in one portion and stirred for 30 min. The THF was then removed by rotary evaporation and the product was extracted into methylene chloride and washed with water and brine. The product thus obtained was purified by flash silica gel chromatography eluting with 10% methanol in methylene chloride, and immediately used in the next step.

2-hydroxypropyl-*p*-nitrophenyl phosphate, sodium salt (5) (HPp^{14}NP)—Ten equivalents of Et_3N•3HF was added to compound 4 obtained as described above, and stirred until the reaction was complete as monitored by TLC. After the starting material had completely disappeared, the reaction was quenched by addition of water and aqueous triethylamine until neutrality was achieved. The excess water was evaporated *in vacuo*. The crude product was passed through an ion exchange column (Sephadex Sp C-25) in the Na^+ form. The water was removed by rotary evaporation. Acetone was added to the crude product and undissolved inorganic salts were removed by filtration. Acetone was evaporated under reduced pressure and the sodium salt of the crude product was dissolved in a minimum amount of water and purified by reverse phase chromatography.[25] The product thus obtained is free of any nitrophenol, and was obtained as a white powder after lyophilization.

NIH-PA Author Manuscript

NIH-PA Author Manuscript

NIH-PA Author Manuscript

The ^{15}N, ^{18}O labeled isotopic isomer was synthesized as shown in Scheme 3.

1-Monomethoxytrityl-1,2-propanediol (6)—The primary hydroxyl group of 1,2-propanediol was protected as the monomethoxy-triphenylmethyl ether. This was accomplished by adding 1.43 g (21 mmol) of imidazole to a stirred, room temperature solution of 2 mL (27 mmol) of 1,2-propanediol and 6.5 g (21 mmol) of monomethoxy-triphenylmethylchloride in 25 mL of dry THF. The product of this reaction (1-momomethoxytrityl-1,2-propanediol, or 1-MeOTr diol) was isolated using centrifugal chromatography (Chromatotron) eluting with 9:1 ethyl acetate:hexanes, yielding **6** (6.32 g, 18.1 mmol) in 86% yield.

1-monomethoxytrityl-2-benzoyl-1,2-propanediol (7)—Compound **6** was esterified with ^{18}O-benzoic acid under Mitsunobu conditions[26] by slow addition of 1.14 mL (5.8 mmol) of DIAD to a solution of 2.22 g of the MeOTr diol (6.3 mmol), 0.800 g of ^{18}-O labeled benzoic acid (6.3 mmol), and 1.66 g of triphenyl phosphine (6.3 mmol) in 20 mL of dry THF at −14° C. After 6h the solution was clear and colorless, and an additional 120 μL of DIAD was added dropwise until the solution retained a slight yellow color. The solution was then allowed to warm to room temperature over 8 h. The reaction mixture was concentrated to about a quarter of its original volume, hexanes (5 mL) was added, and the solution was refrigerated overnight to precipitate byproducts. After filtration, 2.65 g (5.6 mmol, 93% yield) of 1-monomethoxytrityl-2-benzoyl-1,2-propanediol (**7**) was isolated by centrifugal chromatography eluting with (9.5:0.5 ethyl acetate:hexanes).

1-Monomethoxytrityl-2-^{18}O-1,2-propanediol (8)—The benzoyl group of **7** was cleaved by addition of excess (>10 eq) of 1M NaOMe in MeOH to a solution of 2.65g of the diprotected diol **7** in 10 mL of dry methanol (containing a few drops of DMF to aid in dissolution) and stirring at room temperature for one hour. The product 1-MeOTr-2-^{18}O-1,2-propanediol (**8**) was isolated in 90% yield (1.76 g, 5.04 mmol) using centrifugal chromatography (80:20 hexanes:ethyl acetate).

1-Monomethoxytrityl-2-^{18}O-(*t*-butyldiphenylsilyl)-1,2-propanediol (9)—At room temperature, 2.5 g (15 mmol, 3 eq) of silver nitrate was added in small portions to a solution of 1.76 g (5 mmol, 1 eq) of **8** in 20 mL of DMF and 3.89 g (15 mmol, 3 eq) of *t*-butyl-diphenyl silyl chloride. After 3h, the precipitate was filtered and discarded, and the DMF was removed by partitioning the product between 10 mL of CH_2Cl_2 and 250 mL of water three times. After removal of dichloromethane in vacuo, the resulting yellow oil was subjected to centrifugal chromatography (9.8:0.2 hexanes:ethyl acetate). The yield of **9** was not determined before immediate use in the next step.

2-(*t*-butyldiphenylsilyl[^{18}O]oxy)-1-propanol (10)—The monomethoxytrityl group was removed from **9** by stirring in excess 95% acetic acid at room temperature for twelve hours. After that time, 50 mL of water was added and the acetic acid was neutralized by cooling the solution to 0°C and adding small potions of sodium carbonate until bubbling had subsided. The aqueous solution was extracted three times, using 20 mL of CH_2Cl_2 each time, and 2-(*t*-butyldiphenylsilyl[^{18}O]oxy)-1-propanol **(10)** was isolated in 90% yield by centrifugal chromatography using hexanes as eluent. The product was further purified by distillation under vacuum at 110°C yielding 1.23 g of **10** (3.9 mmol, 75% yield) as a light yellow oil.

2-[^{18}O]hydroxypropyl-[^{15}N]-*p*-nitrophenyl phosphate (11)—The triethylammonium salt of HpPNP was then made by slowly adding a THF solution of 835 mg (2.63 mmol, 1.1 eq) of **10** and 1 ml (7.18 mmol, 3 eq) of triethyl amine (the solution was approximately 0.1 M in **10**) to a 0.1M THF solution of 0.612 g (2.39 mmol, 1eq) of [^{15}N]-*p*-nitrophenyl phosphorodichloridate at 0°C. The cold solution was allowed to react for two hours, then the

NIH-PA Author Manuscript

NIH-PA Author Manuscript

NIH-PA Author Manuscript

reaction was stopped and the remaining chloridate hydrolyzed by adding excess water at 0°C. The solution was then extracted with 50 mL of dichloromethane three times. The organic layers were dried over magnesium sulfate and concentrated in vacuo. The resulting tan oil gave very clean proton and ^{31}P NMR spectra (<1% pyrophosphate and <1% triester) and was used without further purification in the next step. The secondary alcohol was then deprotected by stirring in 10 mL (excess) triethylamine/HF complex in THF at room temperature. After three days (monitored by ^{31}P NMR), the triethylammonium salt of **11** was isolated by adding 5 mL of water and extracting 3× using 50 mL of ether. This removed the TBDPSi-F product in the ether layer, but also a small amount of the desired product was lost. The remaining product in the aqueous layer was dried via rotary evaporation to a yellow oil, which was diluted in 85% ethanol and passed through a Sephadex SP-25 cation exchange column in the sodium form. The water was removed by a combination of rotary evaporation followed by lyophilization. Sodium fluoride was precipitated from the resultant yellow oil by addition of acetone followed by filtration. The acetone was removed by rotary evaporation, and the remaining yellow oil was dissolved in water and passed through a short reverse-phase silica gel^{25} column to remove remaining organic contaminants. The water was mostly removed by rotary evaporation at 35° C, and the remainder was lyophilized, leaving a white powder, which proved to be 0.174 g (0.574 mmol, 24% yield from the ^{15}N labeled 4-nitrophenyl phosphorodichloridate) of the sodium salt of **11**. This material was pure by ^{1}H and ^{31}P NMR and these spectra were identical with those of the natural abundance material.

Isotopic isomers **5** and **11** were mixed in proportion such as to reconstitute the natural abundance of ^{15}N, which was verified by isotope ratio mass spectrometry.

Kinetic isotope effect measurements

All KIE trials were conducted in triplicate. Uncatalyzed transesterification trials were conducted in 50 mM CHES buffer at pH 10.1, while catalyzed trials were conducted in HEPES at pH 7.8. A stock 7.9 mM solution of the catalyst **1** was prepared according to a published procedure.[8]

A typical uncatalyzed trial was conducted by stirring 0.0725 mmol of HpPNP in 30 mL of 50 mM CHES buffer maintained at 67°C in a block heater. After 8 h, the reaction vessel was cooled to room temperature, and a 250 μL aliquot was removed and added to 3 mL of HEPES buffer at pH 7.8. The absorption at 400 nm of this diluted aliquot of the reaction mixture was used to calculate the amount of nitrophenol released. Reactions were stopped by acidifying to pH 3–4 using 1N HCl. This was extracted with ether three times to remove the *p*-nitrophenol product. The water layer containing residual HpPNP was then titrated to ~pH 11 using 1M NaOH, and returned to the heat block for a period of 80 h to completely react remaining HpPNP. A diluted aliquot was then assayed for *p*-nitrophenol, and this result, together with the first assay of *p*-nitrophenol, was used to calculate the fraction of conversion when reaction had been stopped. The *p*-nitrophenol liberated from the residual HpPNP was isolated by ether extraction as before.

The ether layers from each fraction were dried over $MgSO_4$, filtered, and evaporated using rotary evaporation. The *p*-nitrophenol was sublimed under vacuum at 95°C onto a cold finger apparatus. One-mg portions of each of sample of sublimed *p*-nitrophenol were transferred to tin capsules for isotope ratio mass spectrometry (IRMS).

A typical catalyzed trial was conducted by mixing 0.0580 mmol of HpPNP with 1.12 mL of the 7.9 mM stock solution of (**1**) and addition to HEPES buffer (pH 7.8) containing $NaNO_3$, yielding a total volume of 53 mL with concentrations of 1.09 mM HpPNP, 0.166 mM (**1**), 28 mM HEPES, and 98 mM $NaNO_3$. This solution was stirred at 40°C for approximately 3.5 h, at which time it was cooled. A 1 mL aliquot was removed from the reaction vessel and placed

NIH-PA Author Manuscript

NIH-PA Author Manuscript

NIH-PA Author Manuscript

in a small test tube to serve as a measure of reaction progress. A 25 μL aliquot from this small test tube was then placed in 3 mL of pH 7.0, 200 mM phosphate buffer to measure the absorption at 400 nm for assay of the amount of *p*-nitrophenol present. The rest of the 1 mL sample was titrated to pH 11 to completely react residual HpPNP, which was then similarly assayed, and the fraction of reaction was calculated from these measurements. Control experiments in the absence of **1** showed that the extent of uncatalyzed hydrolysis was negligible over the reaction times and conditions used for measurement of the KIEs of the catalyzed reactions.

As soon as the 1 mL aliquot was removed, the reaction was stopped by acidifying the remaining solution to pH 3–4 using 1N HCl. The *p*-nitrophenol product was isolated as described for the uncatalyzed reactions. The aqueous layer was subsequently titrated to ~pH 11 using 1M NaOH to completely react remaining HpPNP, followed by isolation of the liberated *p*-nitrophenol. These nitrophenol samples were prepared for isotope ratio analysis in the same manner as for the uncatalyzed trials.

Calculation of equilibrium isotope effect (EIE) for deprotonation of the 2' hydroxyl of HpPNP

The DFT B3LYP[27] functional with the standard 6-31+G(d,p) basis set[28] was used to model EIEs on the deprotonation of *p*-nitrophenol and HpPNP. The polarizable continuum solvent model[29] (PCM) with parameters for water was used. All calculations were carried out in *Gaussian03* electronic structure program[30] using default convergence criteria. A vibrational analysis was performed for each stationary point. All optimized structures were confirmed to have only real frequencies corresponding to minima on the potential energy surface, and the Hessians from these calculations were used in the calculations of EIEs by the conventional transition state theory using the Isoeff program.[31] The M05, M05-2X,[32] M06 and M06-2X[33] functionals were also used to model the EIE; the differences were small, and none gave agreement with experiment that were superior to those obtained using B3LYP.

Results

Demonstration of specific base catalysis

Specific base, rather than general-base, catalysis for the uncatalyzed reaction of HpPNP was demonstrated by measuring the hydrolysis rates of HpPNP in pH 10.1 CHES buffer at concentrations of 25 mM, 50 mM, and 100 mM. The rate constants at each concentration were identical within experimental error (data not shown). This demonstrates that deprotonation of the nucleophilic hydroxyl group occurs in a pre-equilibrium step, and not a general base mechanism in which deprotonation is concerted with nucleophilic attack.

NMR analysis of the reaction products verified that the only reaction under the experimental conditions employed is cyclization, followed by slower hydrolytic ring opening. No direct hydrolysis of the diester to produce *p*-nitrophenol was observed (data not shown).

EIE for deprotonation of HpPNP

The results of the PCM/B3LYP/6-31+G(d,p) calculations for the EIEs on the deprotonation of *p*-nitrophenol are compared with the experimental values[34] in the first two rows of Table 1. The third row presents the calculated EIEs on the deprotonation of HpPNP.

Kinetic isotope effects

Figure 4 shows the HpPNP substrate denoting the positions at which KIEs were measured. Equation 1 or Equation 2 were used to calculate the observed isotope effect either from the nitrogen isotope ratios in the product at partial reaction (R_p) and in the original substrate (R_o), or, from the ratios in the residual substrate at partial reaction (R_s) and R_o, respectively, at the measured fraction of reaction.[35] The observed isotope effects from experiments to

NIH-PA Author Manuscript

NIH-PA Author Manuscript

NIH-PA Author Manuscript

determine ^{18}O KIEs were corrected for the ^{15}N effect and for incomplete levels of isotopic incorporation in the starting material.[36] The independent calculation of each isotope effect using R_p and R_o and using R_s and R_o from equation 1 and equation 2, respectively, provided an internal check of the results. The KIEs calculated from equation 1 and equation 2 agreed within experimental error in all cases, and the six values for each isotope effect were averaged together to give the results in Table 1.

$$\text{isotope effect}=\log\ (1-f)\ /\log\ \left(1-f\left(R_p/R_o\right)\right) \tag{1}$$

$$\text{isotope effect}=\log\ (1-f)\ /\log\ \left[(1-f)\left(R_s/R_o\right)\right] \tag{2}$$

The kinetic isotope effects measured in this study for the reaction of HpPNP catalyzed by **1** and for the specific base hydrolysis are shown in Table 2. Previously reported[38] leaving group KIEs for the cyclization of uridine-3'-*p*-nitrophenyl phosphate are shown in the last column, for comparison with the present data.

Discussion

Contributions to the isotope effects

A number of KIEs have been reported for both enzymatic, uncatalyzed, and metal-catalyzed phosphate ester reactions,[39] which provides a background for the interpretation of the KIEs measured in this study.

Fission of the P-O bond results in negative charge on the leaving group in the transition state. Charge delocalization by resonance involving the nitrogen atom affects the magnitude of ^{15}k. In phosphoryl transfer reactions this isotope effect reaches a maximum of 1.003, implying extensive bond fission and no charge neutralization.[39] Kinetic effects larger than the equilibrium effect for deprotonation arise from differences between the reactant states (phosphoryl group compared to a proton) and from proximity of the leaving group to the anionic phosphoryl group in the transition state, enhancing charge delocalization. The $^{18}k_{lg}$ KIE is a measure of the extent of P-O fission. Its magnitude is small for a transition state with little bond fission to the leaving group, and can reach 1.03 for a loose transition state with nearly complete bond fission.[39]

The observed nucleophile KIEs in Table 2 reflect the fractionation of the oxygen isotopes for deprotonation of the hydroxyl group and the kinetic isotope effect on nucleophilic attack. The latter is composed of the temperature independent factor (TIF) and the temperature dependent factor (TDF).[40,41] The TIF, sometimes called the imaginary frequency ratio, reflects the extent to which the labeled atom participates in the reaction coordinate. This factor always favors the lighter isotope since its imaginary frequency is larger, producing a normal contribution to the isotope effect. The TDF reflects differences in vibrations (bonding) of the labeled atom in the ground state compared to the transition state. Tighter bonding to the labeled atom favors the heavier isotope, and thus results in an inverse contribution to the isotope effect. Nucleophile KIEs are the product of these two contributions, and are generally normal when nucleophile bond formation occurs in the rate-limiting step because the imaginary frequency contribution often dominates.[20,41–44] For these reasons the magnitude of a nucleophile KIE is largest for early transition states and becomes smaller (less normal) as bonding to the nucleophile in the transition state increases. Inverse nucleophile KIEs are possible in late transition states if bond formation is sufficiently far advanced that the inverse contribution from the TDF outweighs

NIH-PA Author Manuscript

NIH-PA Author Manuscript

NIH-PA Author Manuscript

the TIF.[44,45] An observed nucleophile isotope effect will also be inverse in a stepwise mechanism, if nucleophilic attack forms an intermediate and a subsequent step is rate-determining.[18] In such a mechanism the observed nucleophile KIE is, in effect, the equilibrium isotope effect on formation of the intermediate; there is no TIF in this case since there is no imaginary frequency involving the labeled atom in the transition state of the rate-determining step.

The nucleophile KIEs for the uncatalyzed reactions of HpPNP were determined under specific base conditions. Under such conditions the nucleophile is deprotonated in a pre-equilibrium step, which allows for a separation of the individual contributions to the observed KIE from the separate steps of deprotonation and nucleophilic attack. Similarly, the absence of a solvent deuterium isotope effect on the reaction catalyzed by **1** indicates that the nucleophile in the catalyzed reaction is also deprotonated in a pre-equilibrium step.[9]

A precise separation of the two contributions requires knowledge of the equilibrium isotope effect (EIE) for deprotonation. No experimental ^{18}O EIE for the deprotonation of an alcohol has been reported. The deprotonation of water results in a normal ^{18}O EIE of 1.04 (in other words, a 4% enrichment of ^{16}O).[46] However, this fractionation is for the bulk solvent, and includes the ensemble of the hydrated hydroxide molecule and includes secondary contributions from hydrogen bonds between the hydroxide and its solvating waters. Other reported experimental ^{18}O EIEs on deprotonation are those for phosphoric and carboxylic acids, and for *p*-nitrophenol, which range from 1.015 to 1.022.[47]

Ab initio calculations (Table 1) were used to estimate the EIE on the deprotonation of HpPNP. Calculations were also carried out on *p*-nitrophenol as a test of the reliability of the computational method. The PCM/B3LYP/6-31+G(d,p) method gave the best results, overestimating the small secondary ^{15}N EIE for *p*-nitrophenol deprotonation, and predicting an ^{18}O EIE of 1.0127, in reasonably good agreement with the experimental value of 1.0153. Calculated EIEs for the deprotonation of HpPNP are shown in Table 1; a negligible effect at nitrogen is predicted as expected, and an EIE at oxygen of 1.0245.

Another consideration in comparing the nucleophile KIEs in the uncatalyzed and catalyzed reactions of HpPNP is the binding mode of the catalytic complex. This is uncertain, and it is possible that the nucleophilic hydroxide coordinates to one of the zinc ions. Precedent indicates that metal ion coordination would reduce the EIE for deprotonation. For example, the EIE for deprotonation of a water molecule coordinated to Co(III) ion is 1.011, a value obtained from the EIEs between $(NH_3)_5$Co(III)-OH_2 and water (1.0196) and $(NH_3)_5$Co(III)-OH and water (1.008).[48] The weaker Lewis Acid Zn(II) will likely result in a smaller reduction in the EIE than Co(III). Coordination itself will result in a small inverse isotope effect, but reported ^{18}O effects for coordination to zinc ions have been <1%.[16,49]

The uncatalyzed cyclization reaction

The similarity of the leaving group KIEs for the specific-base hydrolysis reactions of HpPNP and uridine-3'-*p*-NPP mirrors the similar Brønsted β_{lg} values for the two respective reactions, and indicates a similar degree of TS bond fission. These two reactions are thus mechanistically similar, indicating that the HpPNP reaction is a good model for the cyclization of uridine-3'-*p*-NPP. In both reactions weakening of the P-O bond is slight. The $^{18}k_{bridge}$ is in the range of values observed for alkaline hydrolysis of diesters of *p*-nitrophenol[39], reactions that have been implicated by LFER data to be concerted. A significant difference is that the alkaline hydrolysis reactions are characterized by normal ^{15}k KIEs. The absence of a significant normal ^{15}k in the cyclization of HpPNP indicates that no appreciable charge develops on the leaving group in the transition state.

NIH-PA Author Manuscript

NIH-PA Author Manuscript

NIH-PA Author Manuscript

If the cyclization is stepwise, then phosphorane formation should be rate-determining with the labile *p*-nitrophenol leaving group, and thus KIEs will reflect this step. X-ray structures show that apical P-O bonds in phosphoranes are slightly longer (by about 0.05 Å) than in phosphate esters.[50] This slight lengthening might account for the pattern of a small $^{18}k_{bridge}$ and the absence of a significant ^{15}k seen in the uncatalyzed reactions. Correction of the observed nucleophile KIE for the calculated EIE on deprotonation gives a $^{18}k_{nuc}$ value of 1.0079. For comparison, the reported $^{18}k_{nuc}$ for attack of hydroxide on the diester thymidine-5'-*p*-nitrophenylphosphate is 1.027 after correction for deprotonation of water.[42] The smaller value in the present reaction suggests greater nucleophilic participation in the transition state. Some of the difference may also arise from the intramolecularity of the HpPNP reaction, which could reduce the reaction coordinate motion of the nucleophilic atom, lowering the TIF component of the isotope effect.[20] In any event, the $^{18}k_{nuc}$ clearly indicates that nucleophilic attack occurs in the rate-determining step. The set of KIEs for the uncatalyzed cyclization of HpPNP are consistent with the rate-determining formation of a phosphorane implied by LFER data discussed earlier, though a concerted reaction with little P-O bond fission in the transition state is not excluded by the data.

The cyclization reaction catalyzed by 1

A different pattern of KIEs is observed for the cyclization of HpPNP catalyzed by the complex **1**. This reaction displays notably larger leaving group KIEs that are one-third to one-half of their maximum values, indicative of significant negative charge accumulation and P-O bond fission, clearly indicating that leaving group departure occurs in the rate-determining step. The observed $^{18}k_{nuc}$ is more than 2% smaller than for the uncatalyzed reaction. Assuming the same EIE correction for deprotonation as for the uncatalyzed reaction yields a corrected $^{18}k_{nuc}$ of 0.9874, implicating a higher degree of nucleophile-phosphorus bond formation in the transition state. Together with the leaving group KIEs, the data indicate a concerted mechanism. An inverse nucleophile KIE can be indicative of rate-determining breakdown of a phosphorane intermediate, but the corrected $^{18}k_{nuc}$ here is much less inverse than the $^{18}k_{nuc}$ of 0.934 reported for the reaction of a cobalt complex for which such a mechanism was concluded.[18]

Could some of the difference in $^{18}k_{nuc}$ arise from zinc-coordination?

There is no direct evidence for nucleophile coordination, and it is proposed that both zinc centers interact with the phosphoryl group in a bridging interaction.[9] The absence of a solvent KIE shows that the nucleophile is deprotonated prior to rate-determining cyclization, so the active complex consists of HpPNP with the 2' hydroxyl nucleophile ionized. Kinetic data are consistent either with ionized HpPNP binding from solution and then reacting, or with the neutral 2'-hydroxyl form of HpPNP binding to the ionized catalyst and undergoing proton transfer (Figure 2).[9] For the sake of completeness, we consider here how Zn coordination to the nucleophile might affect the KIE data. Coordination of this oxygen to zinc should result in an inverse effect, as well as in a smaller EIE for deprotonation. Precedent suggests that the inverse effect for coordination of oxygen to Zn is less than 1%.[16,49] If the EIE for deprotonation is assumed to remain 1.0245, then a coordination EIE of 0.99 gives a corrected $^{18}k_{nuc}$ of 0.997. If the EIE on deprotonation is reduced by half to 1.0123 (probably a generous estimation of the effect of coordination) then the corrected $^{18}k_{nuc}$ becomes 1.009. It is thus theoretically plausible that the difference in $^{18}k_{nuc}$ arises from zinc coordination of the nucleophile, assuming such coordination occurs and that it also significantly affects the EIE on deprotonation. However, the large difference in leaving group KIEs still leads to the conclusion of a different transition state in the two reactions; it is not clear how greater TS bond fission could result solely from phosphoryl coordination to zinc if the nucleophilic participation is unchanged. In our opinion, the difference in $^{18}k_{nuc}$ between the two reactions most likely arises at least in part from greater transition state bond formation in the reaction catalyzed by **1** than in the uncatalyzed reaction.

NIH-PA Author Manuscript

NIH-PA Author Manuscript

NIH-PA Author Manuscript

Uncertainty about the interactions of the substrate-catalyst complex precludes computational modeling using the KIEs to obtain more specific transition state information. Some conclusions can nonetheless be drawn from the data. The observation of significant KIEs in the reaction catalyzed by 1 demonstrates that the chemical step of cyclization is rate-determining. In contrast, the cyclization of HpPNP in methanol solution catalyzed by a similar dinuclear zinc catalyst, but lacking the central bridging alkoxide ligand, proceeds via rate-limiting coordination to the complex.[19] This difference may be solvent-related, or could result from geometric and electrostatic differences in the catalyst resulting from the bridging ligand. A later transition state with greater leaving group bond fission and more nucleophilic bond formation is implied by the KIE data for the cyclization catalyzed by **1** compared to the uncatalyzed reaction.

It is also interesting to compare the results obtained here with a recent study of the cyclization of a similar analog, **12**. This compound has a thiolate leaving group with an estimated pK_a of about 9, not too much higher than that of the *p*-nitrophenyl leaving group of HpPNP. The specific base cyclization of **12** has an uncorrected $^{18}k_{nuc} = 1.025 \pm 0.005$, and $^{34}k_{lg} = 1.0009 \pm 0.0001$.[51] The scissile ester atom is sulfur and not oxygen in this case, and sulfur-34 KIEs are smaller than oxygen-18 KIEs due to the proportionally smaller mass difference. Nonetheless, it is noteworthy that a similar pattern of a very small leaving group KIE and an observed nucleophile KIE in the 2–3% range is observed in both reactions, suggesting a similar mechanism and transition state in both reactions.

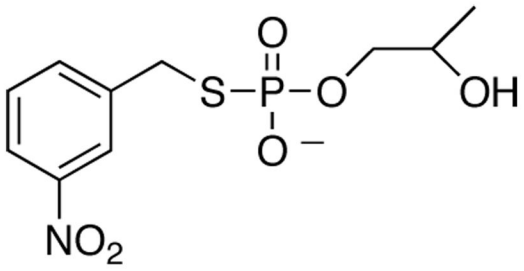

12

Conclusions

The isotope effects demonstrate that the cyclization of HpPNP catalyzed by **1** proceeds with a different transition state than the uncatalyzed reaction. The catalyzed reaction is concerted, with bond formation to the nucleophile and bond fission to the leaving group both significantly advanced in the transition state. The transition state of the uncatalyzed cyclization of HpPNP is earlier in both respects, with less nucleophile bond formation and less bond fission to the leaving group. The KIE data are consistent with the previous conclusion[4] of rate-limiting phosphorane formation for the uncatalyzed reaction, but do not rule out a concerted mechanism.

The results of this study demonstrate the potential for a metal ion-based catalyst using biologically relevant metal ions to select for an altered transition state for phosphoryl transfer. Why does the dinuclear complex stabilize a transition state that is different from that for the uncatalyzed reaction? The rate acceleration observed for the metal ion complex-catalyzed reaction is mainly from electrostatic stabilization of the transition state.[52] This transition state has a charge of −2 for both the uncatalyzed and catalyzed reactions. The main difference

NIH-PA Author Manuscript

NIH-PA Author Manuscript

NIH-PA Author Manuscript

between the transition states for the two reactions is that for the catalyzed reaction there is a greater shift in negative charge away from the nucleophile and onto the leaving group and, possibly, onto the phosphoryl oxygens to a small extent. The observation that the metal-catalyzed reaction proceeds though a more concerted transition state therefore suggests that the catalyst provides preferential stabilization of charge at the latter two sites, compared with the nucleophilic oxygen.

Interestingly, studies of the zinc metalloenzyme alkaline phosphatase have not shown evidence for a change in mechanism or transition state in either its native monoesterase activity or its promiscuous sulfatase activity. Continuing investigations will aid in the understanding of how, and when, the catalytic advantages of metal-assisted catalysis are accompanied by differences in mechanism and/or transition states.

Supplementary Material

Refer to Web version on PubMed Central for supplementary material.

Acknowledgement

The authors are grateful for financial support from the NIH (GM47297) to ACH and NSF (CHE-9986332) to JRM and JPR.

References

1. Davis AM, Hall AD, Williams A. J. Am. Chem. Soc 1988;110:5105–5108.
2. Brown DM, Usher DA. J. Chem. Soc 1965;87:6558–6564.
3. Satoh K, Inoue Y. Chem. Lett 1972:1097–1100. Kosonen M, Youseti-Salakdeh E, Stromberg R, Lonnberg H. J. Chem. Soc. Perkin Trans 1997;2:2661–2666.
4. Lonnberg H, Stromberg R, Williams A. Org Biomol Chem 2004;2:2165–2167. [PubMed: 15280948]
5. Tsang JSW, Neverov AA, Brown RS. J. Am. Chem. Soc 2003;125:1559–1566. [PubMed: 12568616]
6. Iranzo O, Kovalevsky AY, Morrow JR, Richard JP. J. Am. Chem. Soc 2003;125:1988–1993. [PubMed: 12580627]
7. O'donoghue A, Pyun SY, Yang MY, Morrow JR, Richard JP. J. Am. Chem. Soc 2006;128:1615–1621. [PubMed: 16448134]
8. Iranzo O, Elmer T, Richard JP, Morrow JR. Inorg. Chem 2003;42:7737–7746. [PubMed: 14632489]
9. Yang MY, Iranzo O, Richard JP, Morrow JR. J. Am. Chem. Soc 2005;127:1064–1065. [PubMed: 15669821]
10. Hasset A, Blattler W, Knowles JR. Biochemistry 1982;21:6335–6340. [PubMed: 7150563]Knowles J. Annu. Rev. Biochem 1980;49:877–919. [PubMed: 6250450]
11. Herschlag D, Jencks WP. J. Am. Chem. Soc 1987;109:4665–4674.
12. Admiraal SJ, Herschlag D. Chem. & Biol 1995;2:729–739. [PubMed: 9383480]
13. Harrowfield JM, Jones DR, Lindoy LF, Sargeson AM. J. Am. Chem. Soc 1980;102:7733–7741.Jones DR, Lindoy LF, Sargeson AM. J. Am. Chem. Soc 1983;105:7327–7336.
14. Rawlings J, Hengge AC, Cleland WW. J. Am. Chem. Soc 1997;119:542–549.
15. Hollfelder F, Herschlag D. Biochemistry 1995;34:12255–12264. [PubMed: 7547968]Catrina IE, Hengge AC. J Am Chem Soc 2003;125:7546–7552. [PubMed: 12812494]
16. Zalatan JG, Catrina I, Mitchell R, Grzyska PK, O'Brien PJ, Herschlag D, Hengge AC. J. Am. Chem. Soc 2007;129:9789–9798. [PubMed: 17630738]
17. Williams NH, Cheung W, Chin J. J. Am. Chem. Soc 1998;120:8079–8087.Wahnon D, Lebuis A-M, Chin J. Angew. Chem. Int. Ed. Eng 1995;34:2412–2414.
18. Humphry T, Forconi M, Williams NH, Hengge AC. J. Am. Chem. Soc 2002;124:14860–14861. [PubMed: 12475323]

NIH-PA Author Manuscript

NIH-PA Author Manuscript

NIH-PA Author Manuscript

19. Bunn SE, Liu CT, Lu ZL, Neverov AA, Brown RS. J Am Chem Soc 2007;129:16238–16248. [PubMed: 18047345]
20. Cassano AG, Anderson VE, Harris ME. Biochemistry 2004;43:10547–10559. [PubMed: 15301552]
21. Anderson MA, Shim H, Raushel FM, Cleland WW. J. Am. Chem. Soc 2001;123:9246–9253. [PubMed: 11562204]
22. Hengge AC, Cleland WW. J. Am. Chem. Soc 1991;113:5835–5841.
23. O'Leary, MH. Methods Enzymol. Purich, DL., editor. Vol. Vol. 64. New York: Academic Press; 1980.
24. Hengge AC. J. Am. Chem. Soc 1992;114:2747–2748.Hengge AC, Edens WA, Elsing H. J. Am. Chem. Soc 1994;116:5045–5049.
25. Kuhler TC, Lindsten GR. J. Org. Chem 1983;48:3589–3591.
26. Mitsunobu O. Synthesis 1981;1:1–28.
27. Francl MM, Pietro WJ, Hehre WJ, Binkley JS, Gordon MS, Defrees DJ, Pople JA. J Chem Phys 1982;77:3654–3665.Hariharan PC, Pople JA. Theor. Chim. Acta. 1973213-
28. Becke AD. Phys Rev A 1988;38:3098–3100. [PubMed: 9900728]Becke AD. J Chem Phys 1993;98:5648–5652.Lee CT, Yang WT, Parr RG. Phys Rev B 1988;37:785–789.
29. Miertus SSE, Tomasi J. Chem. Phys 1981;55:117–129.
30. Frisch MJTGW, G W, Schlegel HB, Scuseria GE, Robb MA, Cheeseman JR, Montgomery JJA, Vreven T, Kudin KN, Burant JC, Millam JM, Iyengar SS, Tomasi J, Barone V, Mennucci B, Cossi M, Scalmani G, Rega N, Petersson GA, Nakatsuji H, Hada M, Ehara M, Toyota K, Fukuda R, Hasegawa J, Ishida M, Nakajima T, Honda Y, Kitao O, Nakai H, Klene M, Li X, Knox JE, Hratchian HP, Cross JB, Bakken V, Adamo C, Jaramillo J, Gomperts R, Stratmann RE, Yazyev O, Austin AJ, Cammi R, Pomelli C, Ochterski JW, Ayala PY, Morokuma K, Voth GA, Salvador P, Dannenberg JJ, Zakrzewski VG, Dapprich S, Daniels AD, Strain MC, Farkas O, Malick DK, Rabuck AD, Raghavachari K, Foresman JB, Ortiz JV, Cui Q, Baboul AG, Clifford S, Cioslowski J, Stefanov BB, Liu G, Liashenko A, Piskorz P, Komaromi I, Martin RL, Fox DJ, Keith T, Al-Laham MA, Peng CY, Nanayakkara A, Challacombe M, Gill PMW, Johnson B, Chen W, Wong MW, Gonzalez C, Pople JA. Gaussian, Inc.: Wallingford CT. 2008
31. Anisimov V, Paneth P. J. Math. Chem 1999;26:75–86.
32. Zhao Y, Schultz NE, Truhlar DG. J Chem Phys 2005;123:161103. [PubMed: 16268672]
33. Zhao Y, Schultz NE, Truhlar DG. J Chem Theory Comput 2006;2:364–382.Zhao Y, Truhlar DG. Theor Chem Acc 2008;120:215–241.(Erratum: Ibid. 2008, 119, 525)
34. Hengge AC, Cleland WW. J. Am. Chem. Soc 1990;112:7421–7422.Hengge AC, Hess RA. J. Am. Chem. Soc 1994;116:11256–11263.
35. Bigeleisen J, Wolfsberg M. Adv. Chem. Phys 1958;1:15–76.
36. Cleland, WW. Isotope effects in chemistry and biology. Kohen, A.; Limbach, H-H., editors. Boca Raton, FL: CRC Press; 2006. p. 915-930.
37. Northrop, DB. Isotope Effects on Enzyme-Catalyzed Reactions. Cleland, WW.; O'Leary, MH.; Northrop, DB., editors. Baltimore, MD: University Park Press; 1977. p. 122-152.
38. Hengge AC, Bruzik KS, Tobin AE, Cleland WW, Tsai MD. Bioorg Chem 2000;28:119–133. [PubMed: 10915550]
39. Hengge AC. Acc. Chem. Res 2002;35:105–112. [PubMed: 11851388]
40. Melander, L.; Saunders, WH. Reaction Rates of Isotopic Molecules. Robert, E., editor. Malabar, FL: Krieger; 1987.
41. Westaway KC, Fang Y, Persson J, Matsson O. J. Am. Chem. Soc 1998;120:3340–3344.
42. Cassano AG, Anderson VE, Harris ME. J. Am. Chem. Soc 2002;124:10964–10965. [PubMed: 12224928]
43. Marlier JF. J. Am. Chem. Soc 1993;115:5953–5956.Marlier JF, Dopke NC, Johnstone KR, Wirdzig TJ. J. Am. Chem. Soc 1999;121:4356–4363.
44. Paneth P, O'Leary MH. J. Am. Chem. Soc 1991;113:1691–1693.
45. Hogg JL, Rodgers J, Kovach I, Schowen RL. J. Am. Chem. Soc 1980;102:79–85.
46. Green H, Taube H. J. Phys. Chem 1963;67:1565–1566.

NIH-PA Author Manuscript

NIH-PA Author Manuscript

NIH-PA Author Manuscript

47. Rishavy MA, Cleland WW. Can. J. Chem 1999;77:967–977.

48. Hunt HR, Taube H. J. Phys. Chem 1959;63:124–125.

49. Catrina I, O'Brien P J, Purcell J, Nikolic-Hughes I, Zalatan JG, Hengge AC, Herschlag D. J Am Chem Soc 2007;129:9789–9798. [PubMed: 17630738]

50. Timosheva NV, Chandrasekaran A, Holmes RR. Inorg Chem 2006;45:10836–10848. [PubMed: 17173443]Timosheva NV, Chandrasekaran A, Holmes RR. Inorg Chem 2006;45:3113–3123. [PubMed: 16562968]

51. Iyer S, Hengge AC. J. Org. Chem 2008;73:4819–4829. [PubMed: 18533704]

52. Iranzo O, Richard JP, Morrow JR. Inorg. Chem 2004;43:1743–1750. [PubMed: 14989667]Yang MY, Morrow JR, Richard JP. Bioorg Chem 2007;35:366–374. [PubMed: 17434205]

NIH-PA Author Manuscript

NIH-PA Author Manuscript

NIH-PA Author Manuscript

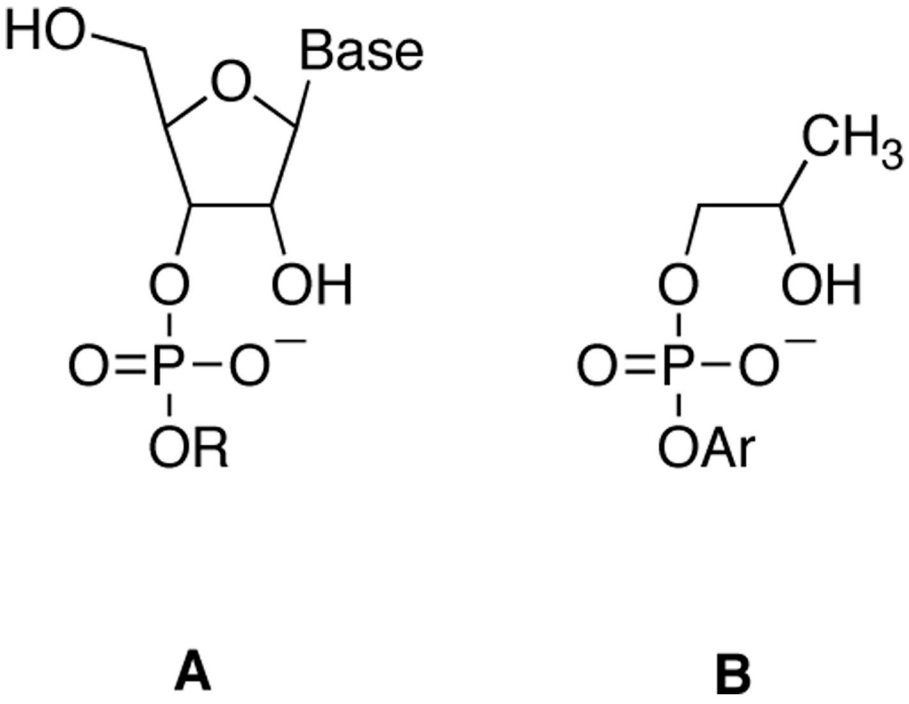

Figure 1.

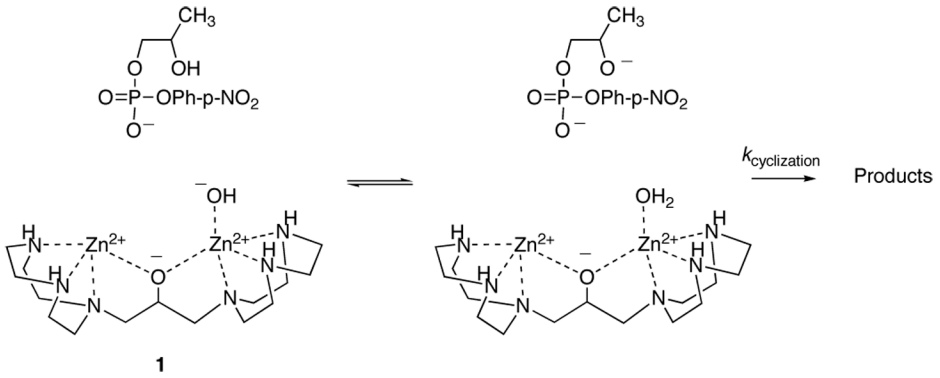

Figure 2.

The mechanism of the cyclization of HpPNP with the catalyst (**1**) concluded from kinetic data. Kinetic data demonstrate that a complex between the substrate and **1** forms; because the binding mode is uncertain, the substrate and catalyst are depicted separately. The Zn-coordinated hydroxide deprotonates the nucleophilic alcohol prior to the nucleophilic step, and the dinuclear Zn center provides transition state stabilization.

NIH-PA Author Manuscript NIH-PA Author Manuscript NIH-PA Author Manuscript

NIH-PA Author Manuscript

NIH-PA Author Manuscript

NIH-PA Author Manuscript

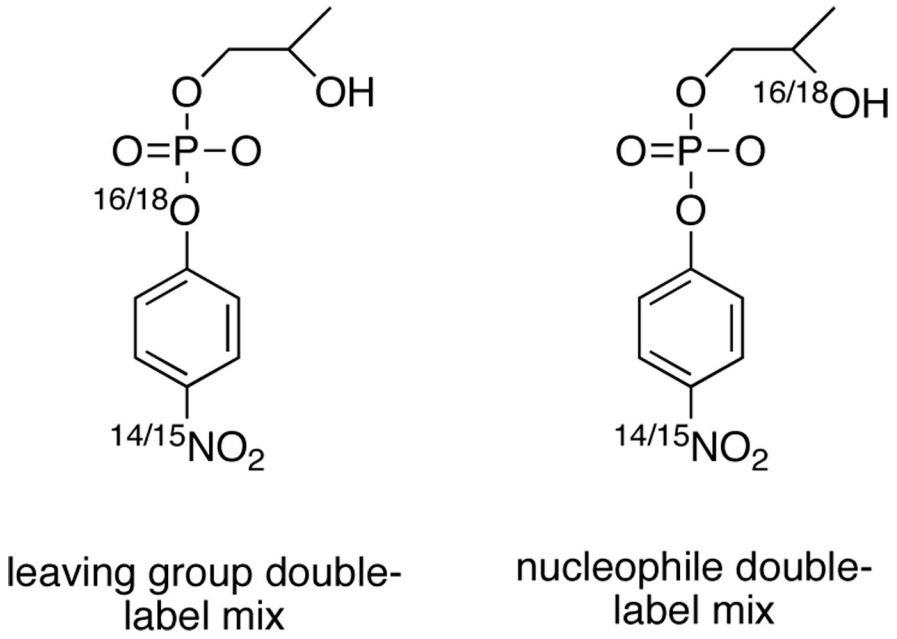

Figure 3.
On the left are shown the isotopic isomers comprising the mixture used for measurement of the isotope effect in the scissile oxygen atom, $^{18}k_{lg}$. On the right, the isomers used for the nucleophile isotope effect, $^{18}k_{nuc}$.

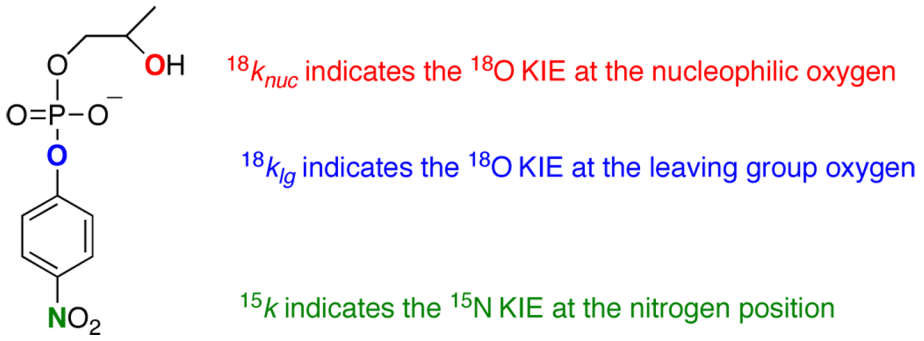

Figure 4.

The positions at which kinetic isotope effects were measured on the reactions of HpPNP. The nomenclature used is the convention[37] in which a leading superscript of the heavier isotope is used to denote the isotope effect on the kinetic quantity. Thus, $^{18}k_{nuc}$ indicates k_{16}/k_{18} , the isotope effect on the rate constant *k* resulting from substitution of ^{18}O for ^{16}O at the nucleophilic position where *k* is the rate constant for the cyclization reaction.

NIH-PA Author Manuscript NIH-PA Author Manuscript NIH-PA Author Manuscript

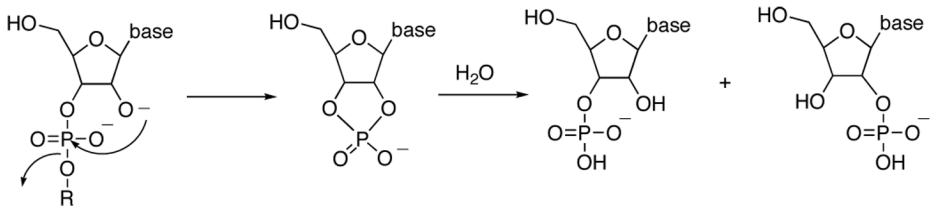

Scheme 1.

NIH-PA Author Manuscript
NIH-PA Author Manuscript
NIH-PA Author Manuscript

NIH-PA Author Manuscript

NIH-PA Author Manuscript

NIH-PA Author Manuscript

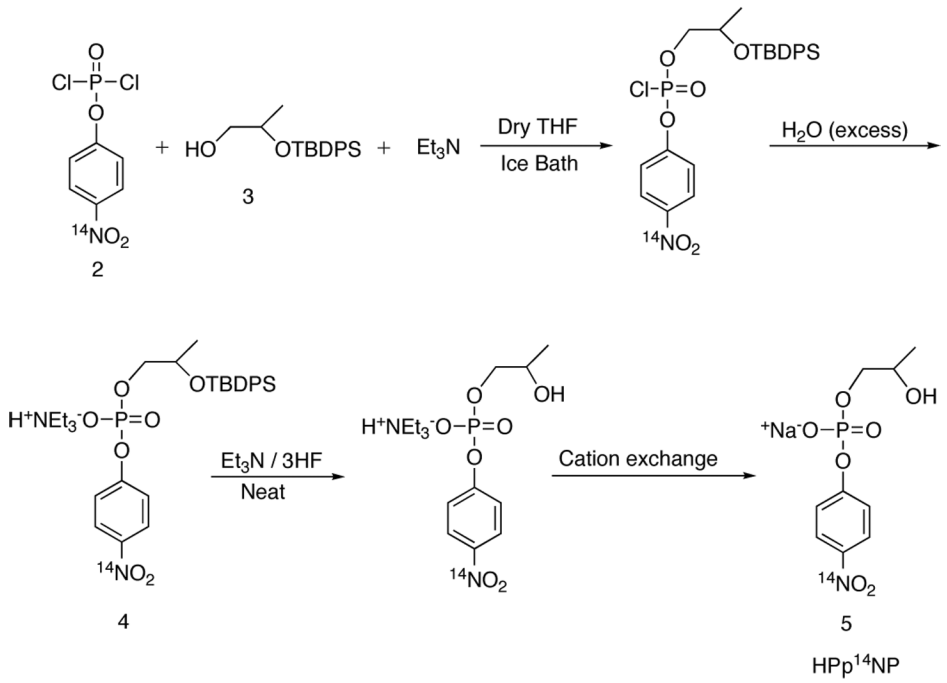

Scheme 2.

NIH-PA Author Manuscript

NIH-PA Author Manuscript

NIH-PA Author Manuscript

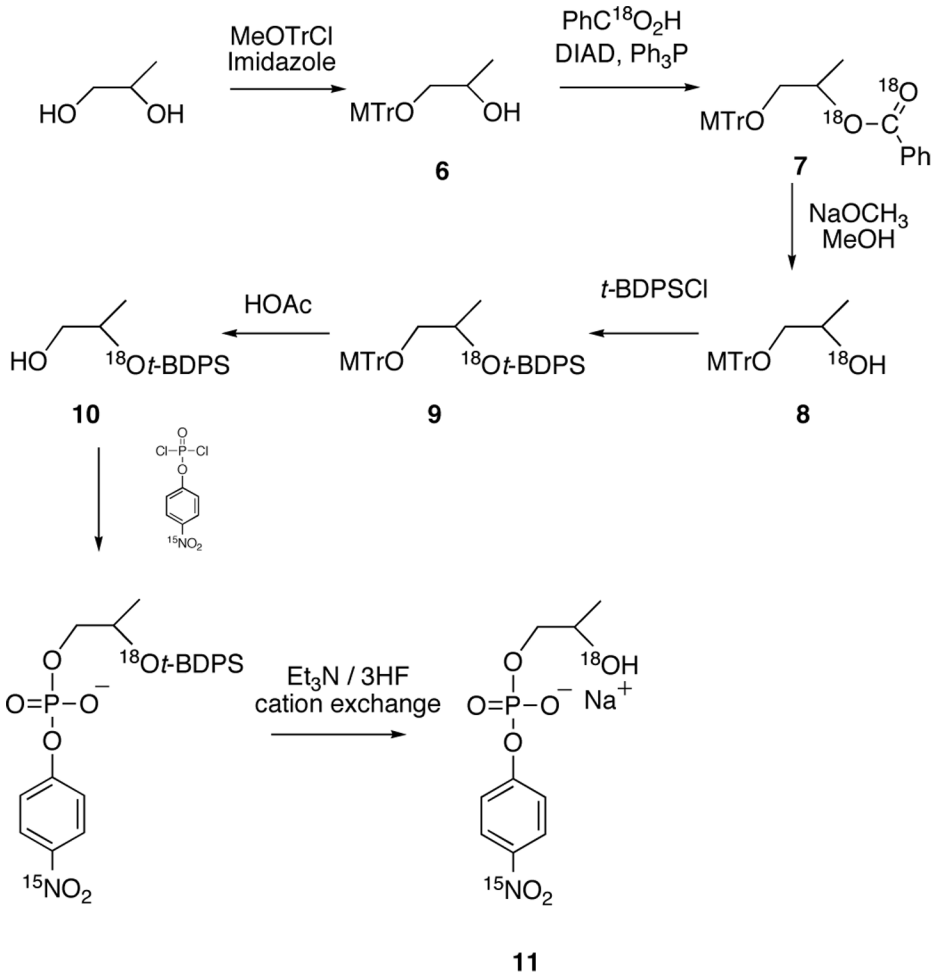

Scheme 3.

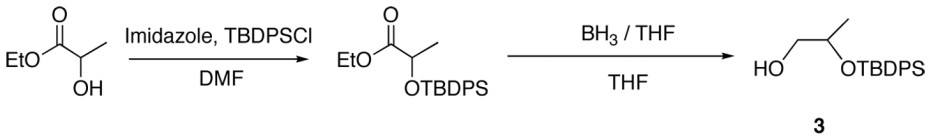

3

Scheme 4.

NIH-PA Author Manuscript
NIH-PA Author Manuscript
NIH-PA Author Manuscript

NIH-PA Author Manuscript

NIH-PA Author Manuscript

NIH-PA Author Manuscript

Table 1

Summary of EIE calculations for deprotonation of *p*-nitrophenol and of HpPNP

Deprotonation	^{15}N-EIE	^{18}O-EIE
p-nitrophenol (B3LYP)	1.0050	1.0127
p-nitrophenol (experiment)	1.0023	1.0153
HpPNP	1.0002	1.0245

NIH-PA Author Manuscript

NIH-PA Author Manuscript

NIH-PA Author Manuscript

Table 2

KIE results for the catalyzed and uncatalyzed reactions of HpPNP and for the uncatalyzed reaction of uridine-3'-*p*-nitrophenyl phosphate. Standard errors in the last decimal place(s) are shown in parentheses. The observed nucleophile KIEs ($^{18}k_{nuc}$) are the product of the effect for deprotonation and the effect for nucleophilic attack, as discussed in the text. The corrected nucleophile KIEs were obtained by correcting the observed values for the calculated EIE for deprotonation of HpPNP. ND = not determined.

	HpPNP Catalyzed by 1	HpPNP specific base hydrolysis	Uridine-3'-*p*-NPP specific base hydrolysis [38]
^{15}k	1.0015 (5)	1.0002 (2)	1.0001 (2)
$^{18}k_{lg}$	1.0113 (5)	1.0064 (9)	1.0059 (9)
Observed $^{18}k_{nuc}$	1.0116 (10)	1.0327 (8)	ND
Corrected $^{18}k_{nuc}$	0.9874	1.0079	ND